Contents lists available at ScienceDirect

Atmospheric Environment: X

Characterization and source identification of PM$_{2.5}$ during intense haze episodes in an urban environment of Lahore

Saima Mohyuddin [a], Khan Alam [b], Bahadar Zeb [c], Muhammad Fahim Khokhar [d], Kaleem Anwar Mir [e], Anthony S. Wexler [f], Ehtiram ul Haq [g], Muhammad Ikram [a,**], Imran Shahid [h,*]

[a] *Department of Physics, Hazara University Mansehra, Mansehra, 21300, Pakistan*
[b] *Department of Physics, University of Peshawar, Peshawar, 25120, Pakistan*
[c] *Department of Mathematics, Shaheed Benazir Bhutto University Sheringal Dir (Upper), 18000, Pakistan*
[d] *Institute of Environmental Sciences and Engineering, National University of Sciences and Technology, Islamabad, 44000, Pakistan*
[e] *Ministry of Climate Change and Environmental Coordination, Islamabad, 44000, Pakistan*
[f] *Department of Civil and Environmental Engineering, University of California, Davis, CA, 95616, USA*
[g] *Department of Basic Sciences and Islamiat, University of Engineering and Technology, Peshawar, Pakistan*
[h] *Environmental Science Centre, Qatar University, PO BOX 2713, Doha, Qatar*

ARTICLE INFO

ABSTRACT

In the backdrop of persistent haze occurrences affecting Southeast Asia and Pakistan's environmental landscape, this study delves into an in-depth analysis of atmospheric Particulate Matter (PM2.5) during intense haze episodes prevalent in Lahore throughout October, November, and December 2019. Employing advanced analytical techniques encompassing Scanning Electron Microscopy (SEM) coupled with Energy-Dispersive Spectroscopy (EDX), X-ray Diffraction (XRD), and Raman Spectroscopy (RS), this investigation meticulously scrutinized PM2.5 samples. The findings showcased substantial variability in PM2.5 concentrations, peaking notably in December within the range of 43.2–301 μgm^{-3}, averaging 168 $\pm$ 88.3 μgm^{-3}, whereas lower concentrations ranging from 30.9 to 268 μgm^{-3}, with an average of 106 $\pm$ 66.1 μgm^{-3}, were observed in October. These concentrations displayed correlations with meteorological parameters, demonstrating a direct association with relative humidity and varying relationships with temperature and wind speed. The maximal PM2.5 concentrations aligned with lower temperatures (19.1 °C), while higher temperatures (26.1 °C) coincided with the lowest concentrations, illustrating distinct relationships with relative humidity percentages and wind speeds. Advanced spectroscopic analyses (RS and XRD) confirmed the presence of various minerals and elements within PM2.5 samples, encompassing calcite, calcium aluminosilicate, hematite, barite, quartz, gypsum, organic carbon, and nineteen elements identified by EDX. Morphological evaluations unveiled diverse particle shapes, from round, pointed, and irregular to rod-like, and agglomerate structures. SEM investigations delineated distinctive groups of anthropogenic and geogenic particles, emphasizing emission sources such as automobile emissions, crop residue burning, biomass burning, construction activities, soil dust, and industrial emissions. This comprehensive study lays the groundwork for source apportionment, vital for understanding consequential impacts on climate, visibility, and human health, fostering future investigations in this domain.

1. Introduction

Air pollution is a complex assemblage of gases and particulate matter, comprising both natural and anthropogenic sources (Ristovski et al., 2012; Kumar et al., 2019). Particulate Matter (PM) originates directly from diverse origins, including natural sources such as dust, sea salt, and emissions from anthropogenic activities termed as primary and secondary emissions (Zhang et al., 2015). Key sources of primary particulates and gaseous precursors, notably nitrogen oxides, sulfur dioxide, and volatile organic compounds, are industrial and vehicular emissions

---

* Corresponding author.
** Corresponding author.
E-mail addresses: mikphysics@gmail.com (M. Ikram), ishahid@qu.edu.qa (I. Shahid).
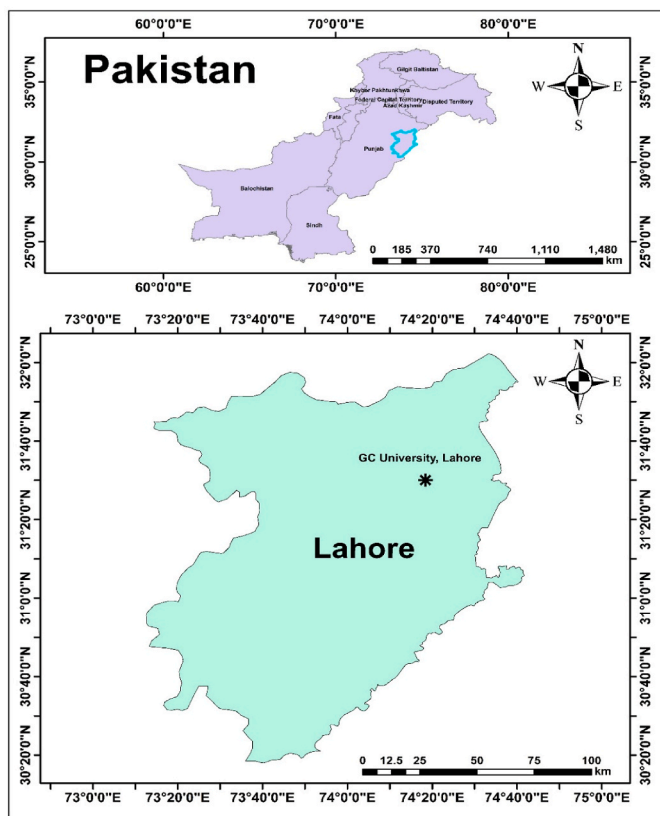
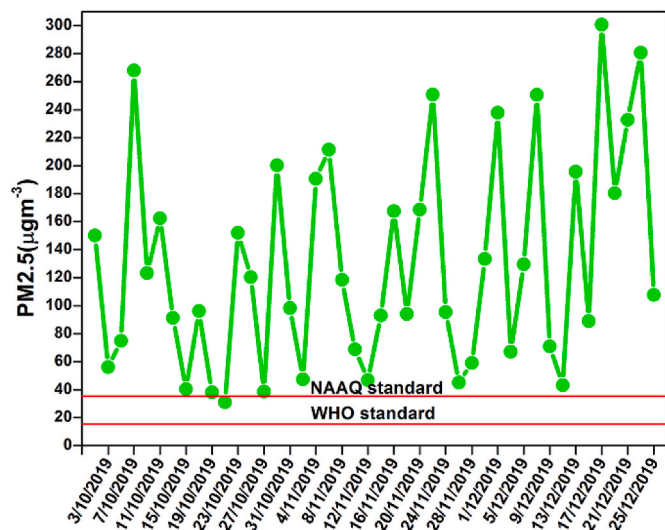Fig. 1. Map of Lahore, including the sampling location.

Fig. 2. Daily variation in PM2.5 mass concentrations during the study period. Comparison of $PM_{2.5}$ concentration with National Ambient Air Quality Standard (NAAQ) and World Health Organization (WHO).

(Rani et al., 2011). PM is a vital pollutant that has affected human health in the past decade, which comes in various sizes based on aerodynamic diameter and can be classified into three main types: coarse PM (PM10–2.5), fine PM (PM2.5) and ultrafine PM (PM0.1) (Inerb et al., 2022; Samae et al., 2021). The chemical composition of PM is contingent upon emission sources and geographical locations (Park and Kim, 2005), comprising inorganic salts, iron compounds, organic carbon, and trace amounts of hazardous metals like chromium, arsenic, cadmium, and lead (Bari and Kindzierski, 2016). These metals, including Cr, As, Ba, Ni,

and P, pose adverse effects on human health and contribute to climate change (Olawoyin et al., 2018).

Particulate matter, especially black carbon within PM2.5, exerts a profound influence on the climate system by directly impacting solar radiation transmission and absorption (Wang et al., 2018). It also serves as cloud condensation nuclei (CCN), indirectly influencing atmospheric processes (Jin et al., 2005). The composition of PM2.5, consisting of carbon aerosols, significantly affects solar radiation absorption and diffusion, ultimately impacting the hydrological cycle (Ramanathan et al., 2005). Additionally, mineral dust present in PM2.5 contributes substantially to the total atmospheric aerosol loading (Rodríguez et al., 2002). Furthermore, PM2.5 is intricately linked to various human health issues, including respiratory and cardiovascular ailments, reduced visibility, and long-term mortality risks (Pun et al., 2017; Dominici et al., 2006). Its primary sources, such as traffic emissions, biomass burning, and agricultural activities, perpetuate health-related concerns (Nihalani et al., 2020).

In Pakistan, environmental challenges due to escalating air pollution are prevalent (Mir et al. 2022, 2023), particularly in regions experiencing fog and mist episodes, notably the southern Himalayan slopes during October and November (Zeb et al., 2018; Alam et al., 2018). Haze episodes, attributed to particulate matter and gaseous pollutants under specific meteorological conditions, stem largely from anthropogenic sources, rapid industrialization, urbanization, and unregulated vehicle emissions. These events pose substantial public health risks, exacerbating pulmonary and cardiovascular diseases. The city of Lahore, specifically, grapples with severe air quality issues. Reports reveal alarmingly high PM2.5 concentrations, surpassing WHO and NAAQS standards, primarily originating from sources like soil/road dust, industrial emissions, vehicular emissions, biomass burning, and secondary aerosols (Ahmad et al., 2021). However, comprehensive characterization and source identification of fine particulates in this region remain limited yet crucial for formulating effective air quality management strategies.

In this context, this study aims to provide a comprehensive understanding of the characteristics and potential sources of PM2.5 during intense haze episodes observed in Lahore's highly polluted urban environment in October, November, and December 2019. Given the escalating concerns over haze-related impacts, especially in densely populated urban centers, an in-depth analysis of PM2.5 becomes imperative. This investigation utilized advanced analytical techniques, including Scanning Electron Microscopy (SEM) coupled with Energy-Dispersive Spectroscopy (EDX), X-ray Diffraction (XRD), and Raman Spectroscopy (RS), to scrutinize PM2.5 samples collected during the identified haze episodes. The study sought to elucidate the temporal variability of PM2.5 concentrations, their correlation with meteorological parameters, and the comprehensive characterization of PM2.5 components, including minerals, elements, and particle morphology.

The significance of this research lies in its potential to unveil the intricacies of PM2.5 dynamics during haze events in an urban setting. The study aims to bridge existing knowledge gaps, in research concerning the dynamics of air pollution in a region where investigations have been relatively limited, contribute valuable insights into the characterization of PM2.5 during intense haze episodes, and delineate potential strategies for mitigating the adverse effects associated with urban haze occurrences. The subsequent sections of this paper are structured as follows: Section 2 details the methodology, covering study site description, sample collection, mass concentration determination, sampling site meteorological conditions, and instrumentation. Section 3 includes an in-depth analysis of PM2.5 concentrations, meteorological conditions, Raman Analysis, and SEM-EDX results. Section 4 provides a concise summary of key findings and their implications.
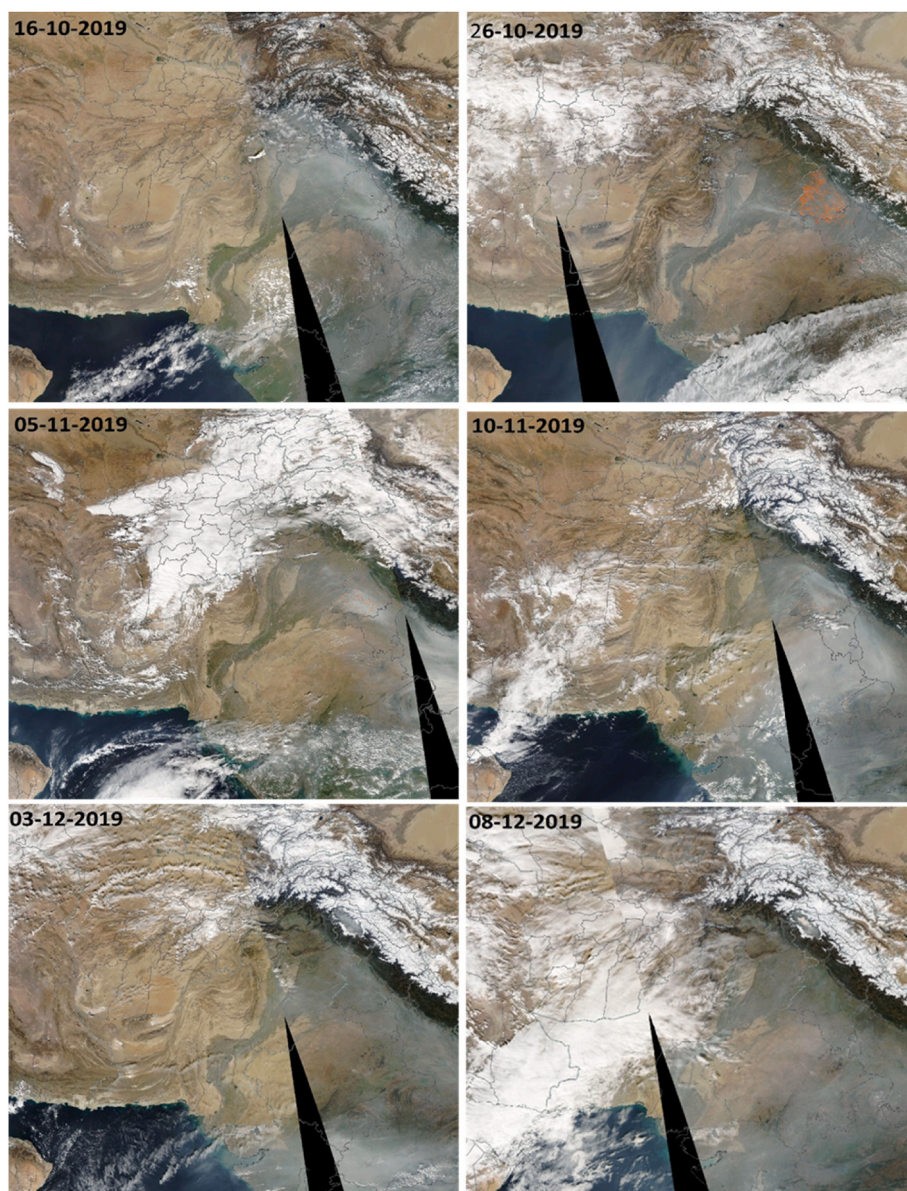
Fig. 3. MODIS true color imagery for various dates during October–December 2019. (For interpretation of the references to color in this figure legend, the reader is referred to the Web version of this article.)
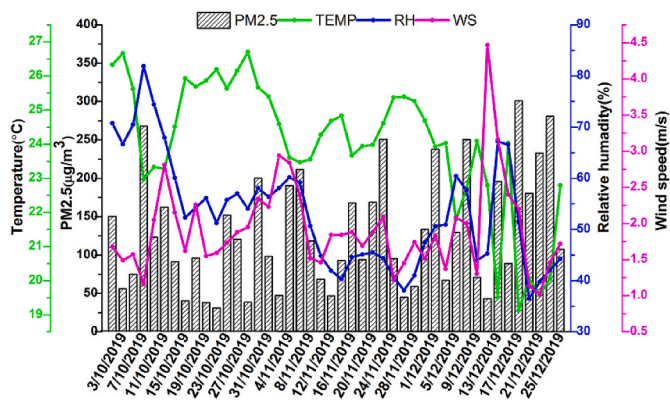

Fig. 4. Meteorological conditions of the study area.

2. Methodology

2.1. Description of the study area (Lahore's urban environment)

Lahore (31°52″ N; 74°35′ E) stands as one of the most densely populated cities in Asia, as delineated in Fig. 1. Covering an expanse of 404 square kilometers, it serves as Pakistan's second-largest commercial and industrial hub. The city has undergone rapid urbanization over recent decades. According to the 2017 census data from the Pakistan Bureau of Statistics (https://www.pbs.gov.pk/content/final-results-census-2017), Lahore's total population surged to 11.1 million with a population density soaring to 628 thousand individuals per square kilometer. This population growth significantly contributes to the escalation of air pollution in metropolitan areas (Che et al., 2023).

Furthermore, the neighboring Punjab region, where Lahore is situated, witnesses extensive rice cultivation, often leading to the burning of residual crops during autumn. This practice has been identified as a key contributor to air quality degradation (Singh and Kaskaoutis, 2014; Alam et al., 2018; FAO, 2018; Mir et al., 2022). Additionally, the city's
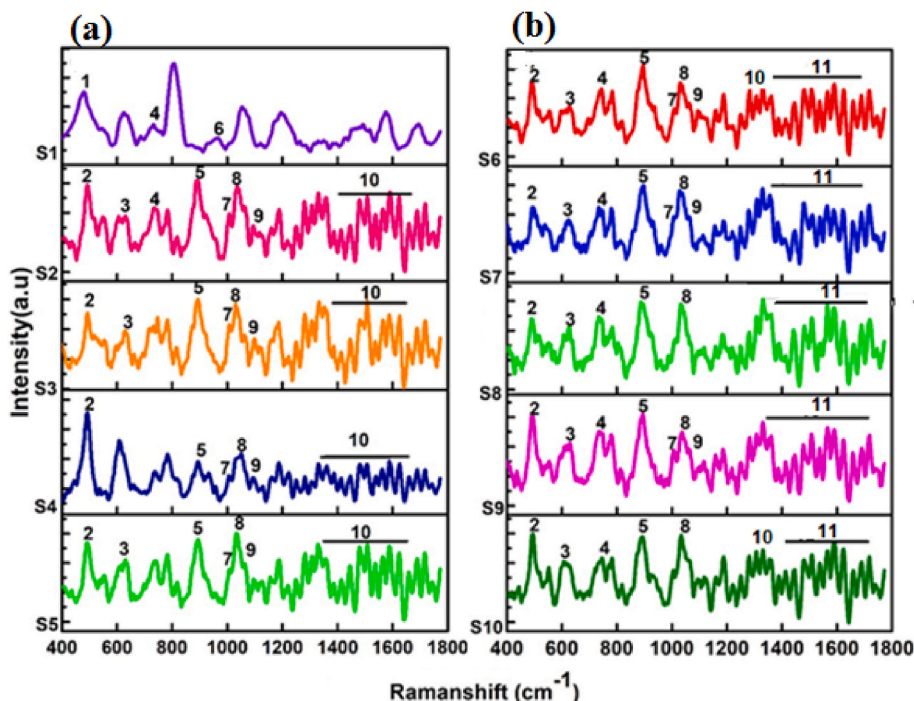
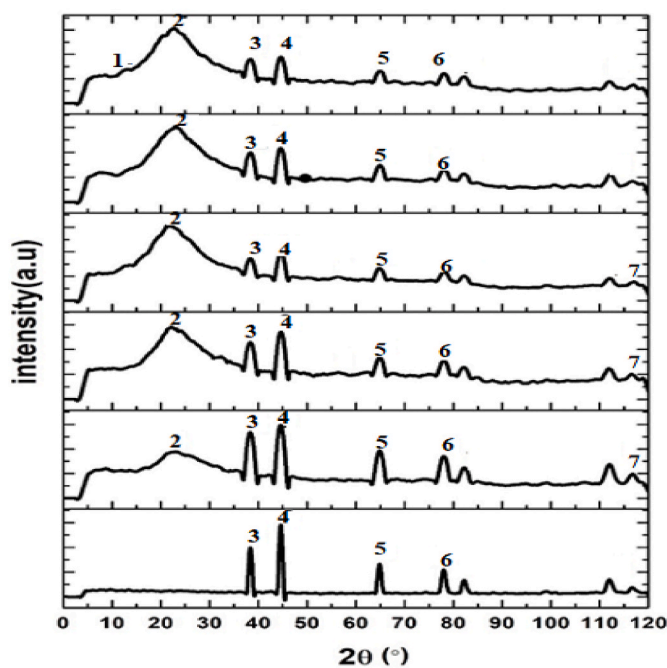**Fig. 5.** Raman spectral images of $PM_{2.5}$ Samples.

Fig. 6. XRD pattern of average values of $PM_{2.5}$ samples.

continuous expansion, amplified industrialization, and various anthropogenic undertakings have collectively culminated in extensive pollution. Vehicular emissions, in particular, stand out as a major factor compromising the atmospheric quality (Alam et al., 2014).

2.2. Sample collections

The quantification of PM2.5 was conducted using a Low-Volume Sampler (LVS) mechanism. Quartz fiber filter substrates served as the collection medium for PM2.5, and a total of 45 samples were
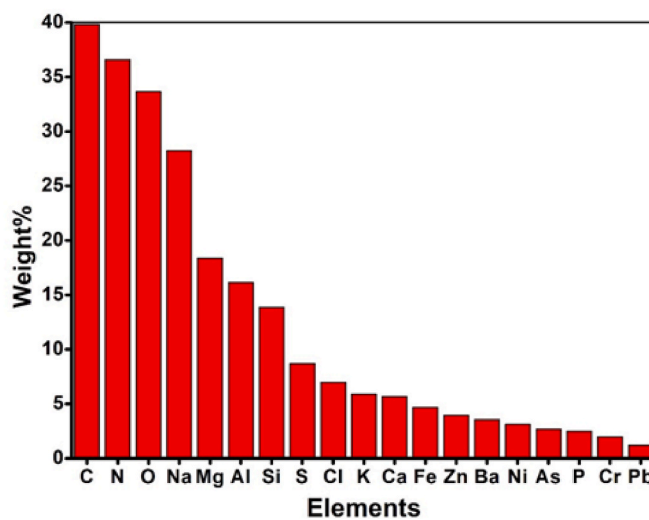

Fig. 7. The average weight percent of individual elements in the study area.

systematically gathered on alternate days over 24 h from 8 a.m. to 8 a.m. throughout October, November, and December 2019. The sampling took place atop the Government College University Lahore premises, positioned at a 5-m elevation above ground level to ensure optimal collection conditions.

Operated consistently at a flow rate of 16 L/min, the LVS method utilized a 47 mm quartz fiber filter possessing a pore size of 0.4 μm for efficient PM2.5 retentions. Following collection, rigorous handling procedures were employed for the filters. Specifically, forceps were delicately used to extract the PM-laden filters, carefully placing them in petri dishes. These samples were then weighed, conditioned, and meticulously stored in a refrigerated environment at 4 °C to forestall heat-induced degradation and prevent the evaporation of volatile materials, preserving their integrity for subsequent evaluations.

Subsequent to the collection phase, the gravimetric mass of the PM2.5 samples was determined using a microbalance. The initial mass
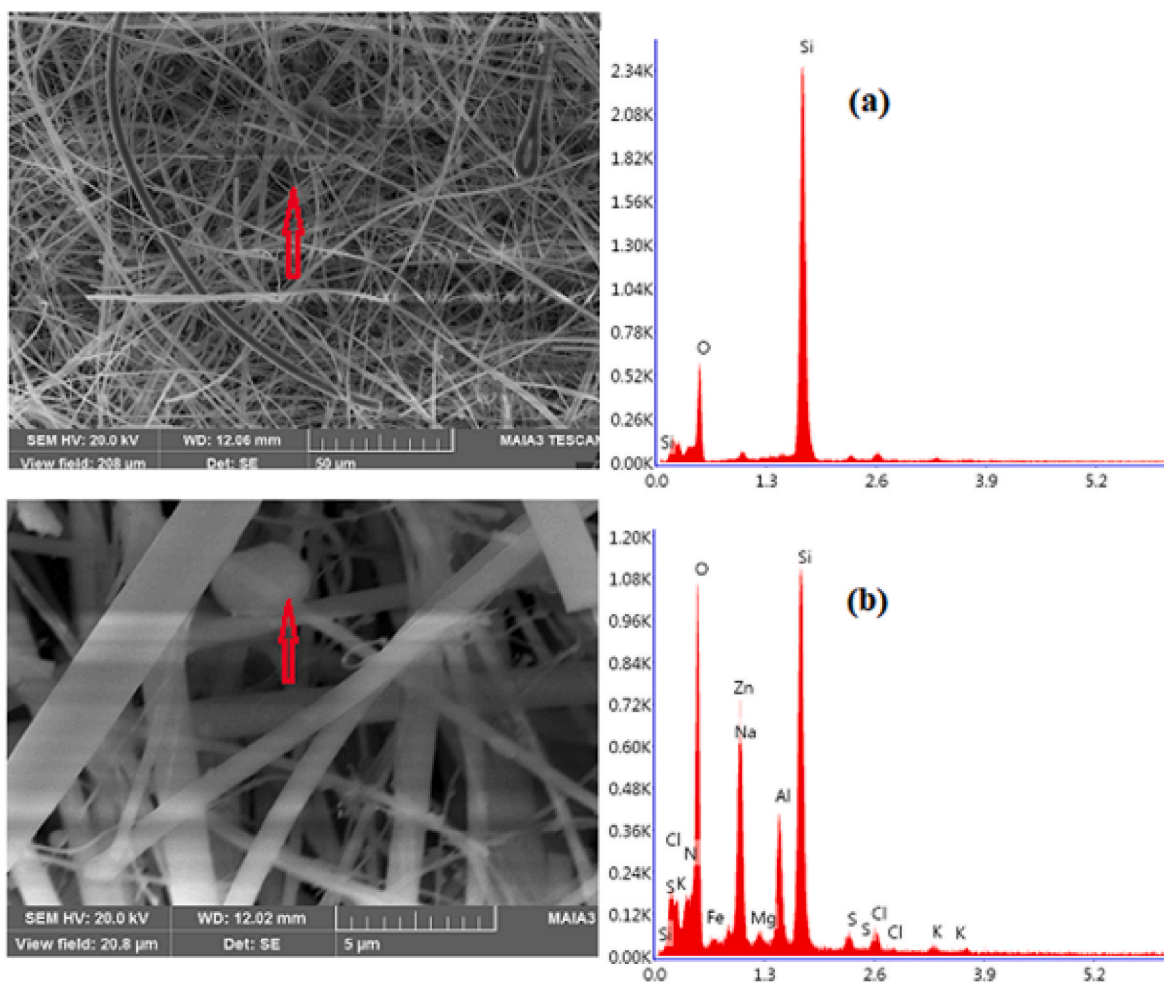
Fig. 8. (a) Quartz-filter (b) Almandine, irregular (c) Ca–Mg-Aluminosilicates, irregular (d) Carbonaceous-particle, agglomerated shape (e) Sulfur-rich particle, capsule shape (f) Barium-particle (g) Nitrogen-rich particles (h) Aluminosilicates-particle.

of the blank filter was subtracted from the final mass of the sampled filter to ascertain the precise mass of PM2.5 collected.

2.3. Determination of mass concentration

The mass concentration (M) of PM2.5 in the air (μg/m^3) was computed using the formula:

$$M = (W_f - W_i) / Q \times t$$

Where M represents the average mass concentration of PM2.5 in the air (μgm^{-3}), W_f and W_i indicate the final and initial average mass of the Quartz filter (μg), Q represents the airflow rate in the sampler (L/min), and t denotes the sampling time (min).

To ensure accuracy, meticulous attention was given to the Quality Assurance and Quality Control protocols throughout the data collection and analysis process. Filters were thoroughly inspected for any defects both before and after the sampling sessions.

2.4. Metrological conditions of the sampling site

The meteorological conditions prevailing at the study site, including temperature, relative humidity (RH), and wind speed (WS), along with their correlations with PM2.5 concentrations, are graphically represented in Fig. 4. The meteorological data were procured from NASA's website (https://power.larc.nasa.gov/data-access-viewer/). Temperature and relative humidity measurements were obtained at distances of

2 m, while wind speed was recorded at 10 m, utilizing the MEERA-2 satellite for the period spanning October to December 2019 over Lahore. Throughout the study period, temperatures varied from 19.1 °C (December) to 26.7 °C (October), with a mean temperature of 24 °C. Relative Humidity (RH) ranged from 36.0% to 81.9%, averaging 53.4%. The minimum recorded wind speed was noted in October (1.10 m/s), while December exhibited the highest speed (4.40 m/s), with an average of 1.90 m/s.

2.5. Instrumentations

2.5.1. Scanning electron microscope with Energy Dispersive X-rays (SEM-EDX)

A Scanning Electron Microscope coupled with Energy Dispersive X-rays (SEM-EDX) was employed to scrutinize the morphology, microstructure, and composition of the particles within the samples. The examination of sample morphology was conducted using a TESCAN MAIA3 field emission scanning electron microscope (FE-SEM). SEM characterization was performed in a high vacuum at appropriate voltages, while EDX analyses were executed at an acceleration voltage of 20 KeV.

The process involves accelerating a focused beam of high-energy electrons ranging from 1 to 40 KeV onto the specimen's surface. This examination yields data concerning surface morphology, grain size, and grain boundaries. The SEM apparatus comprises an electron gun, detectors, a vacuum system, and a scanning system. As the scanned
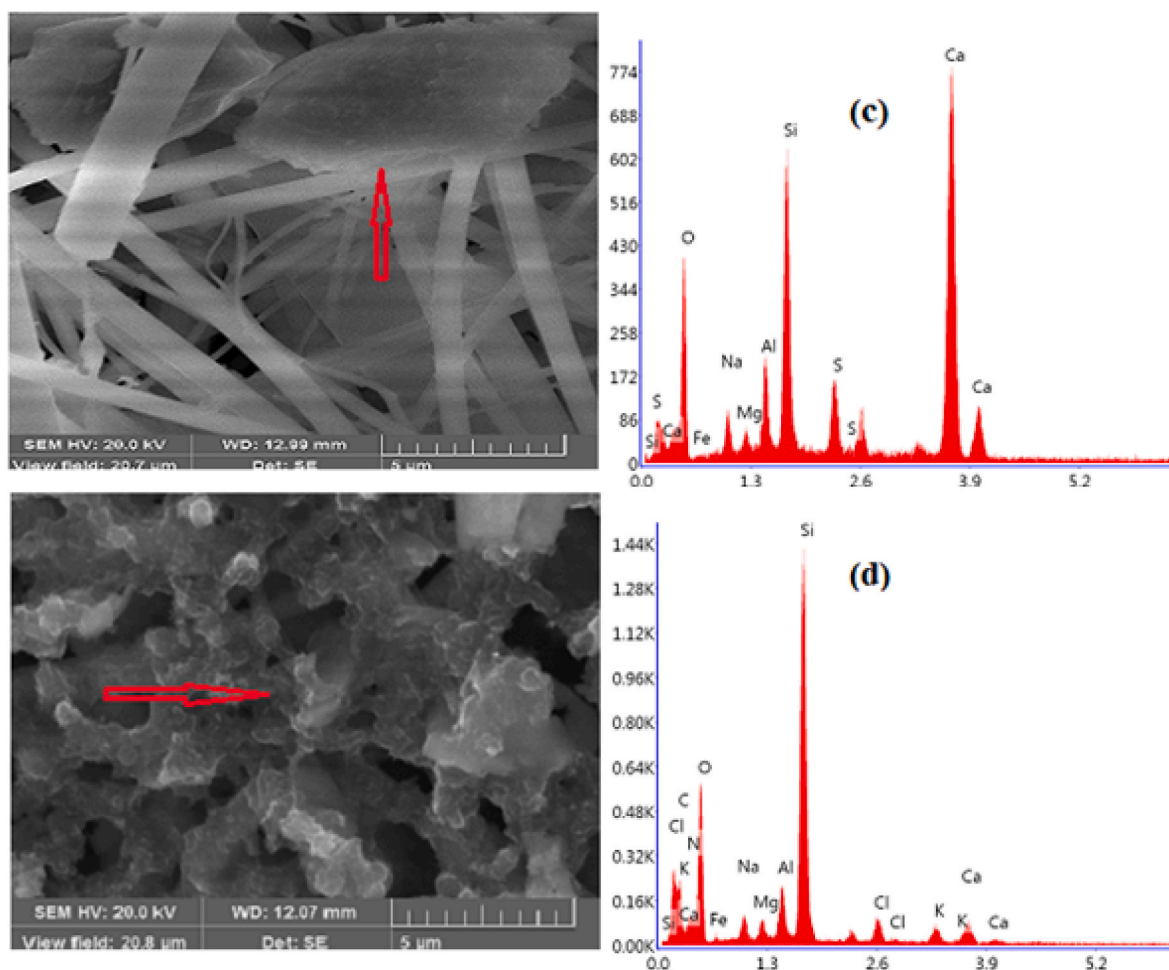
Fig. 8. (*continued*).

electron beam interacts with the specimen's surface, characteristic X-rays, secondary electrons, and backscattered electrons are generated. Both backscattered and secondary electrons are utilized to generate images. Notably, backscattered electrons contribute to phase distribution and atomic number contrast due to the heavier elements scattering more electrons than lighter ones (Vernon-Parry, 2000).

2.5.2. X-ray diffraction

X-ray Diffraction (XRD) serves as a fundamental technique for determining a sample's crystal structure in various forms such as thin films, powder, or solids. It involves the production of X-rays (wavelength 0.1 Å to 5 Å) by a highly energetic electron beam colliding with a metal target accelerated through a potential difference of 60 kV (Lee, 2017). The resulting X-ray spectrum typically comprises different k lines, including kα and kβ X-ray photons. During the diffraction process at an angle "θ," the diffracted X-rays are collected at the detector, and their intensity is plotted against the scattering angle (2θ). This analysis offers insights into the sample's phase constitution, lattice constants, and crystal structure by evaluating the diffraction patterns generated.

2.5.3. Raman Spectroscopy

Raman Spectroscopy (RS) involves the measurement of wavelength and intensity of inelastically scattered light from samples. Among various spectroscopic techniques for the chemical characterization of PM, RS stands as a prominent method that integrates analytical capabilities with an optical microscope, providing spatially resolved compositional information at the micron level (Cardell and Guerra, 2016). Raman spectra also offer valuable information about potential PM sources (Carrero et al., 2014). This technique exposes the sample to monochromatic light, commonly laser light, causing the absorption and re-emission of photons. The energy loss of the re-emitted photons corresponds to the material's vibrational and rotational energy states. In this study, a Raman shift range from 400 cm^{-1}–2000 cm^{-1}, with an exposure time of 30 s and spectral resolution of 1 cm^{-1}, was employed. Scans were conducted at three different points for each sample, and average Raman intensity values were plotted against wavelengths.

3. Results and discussion

3.1. PM_{2.5} concentration and meteorological conditions

Throughout the study period, the PM2.5 concentrations exhibited a significant fluctuation, ranging from 30.9 to 301 μgm^{-3}. Lower concentrations were observed in October, averaging 106 μgm^{-3}, while higher concentrations were recorded in December, averaging 168 μgm^{-3} (Fig. 2). These concentrations considerably exceeded the WHO's recommended daily limit of 25 μgm^{-3}, indicating compromised air quality in Lahore (Kobza et al., 2018). Biomass burning, a common practice in the nearby agricultural areas, especially between October and December, significantly contributes to the elevated PM2.5 levels. Agricultural residues, often burned after harvest, release numerous smoke particles into the atmosphere. Moderate Resolution Imaging Spectro-radiometer (MODIS) data depicted these smoke particles, spread across India and Pakistan, significantly affecting air quality (Fig. 3). These particles, detected by MODIS, indicated widespread biomass burning and agricultural fires, exacerbating the regional air
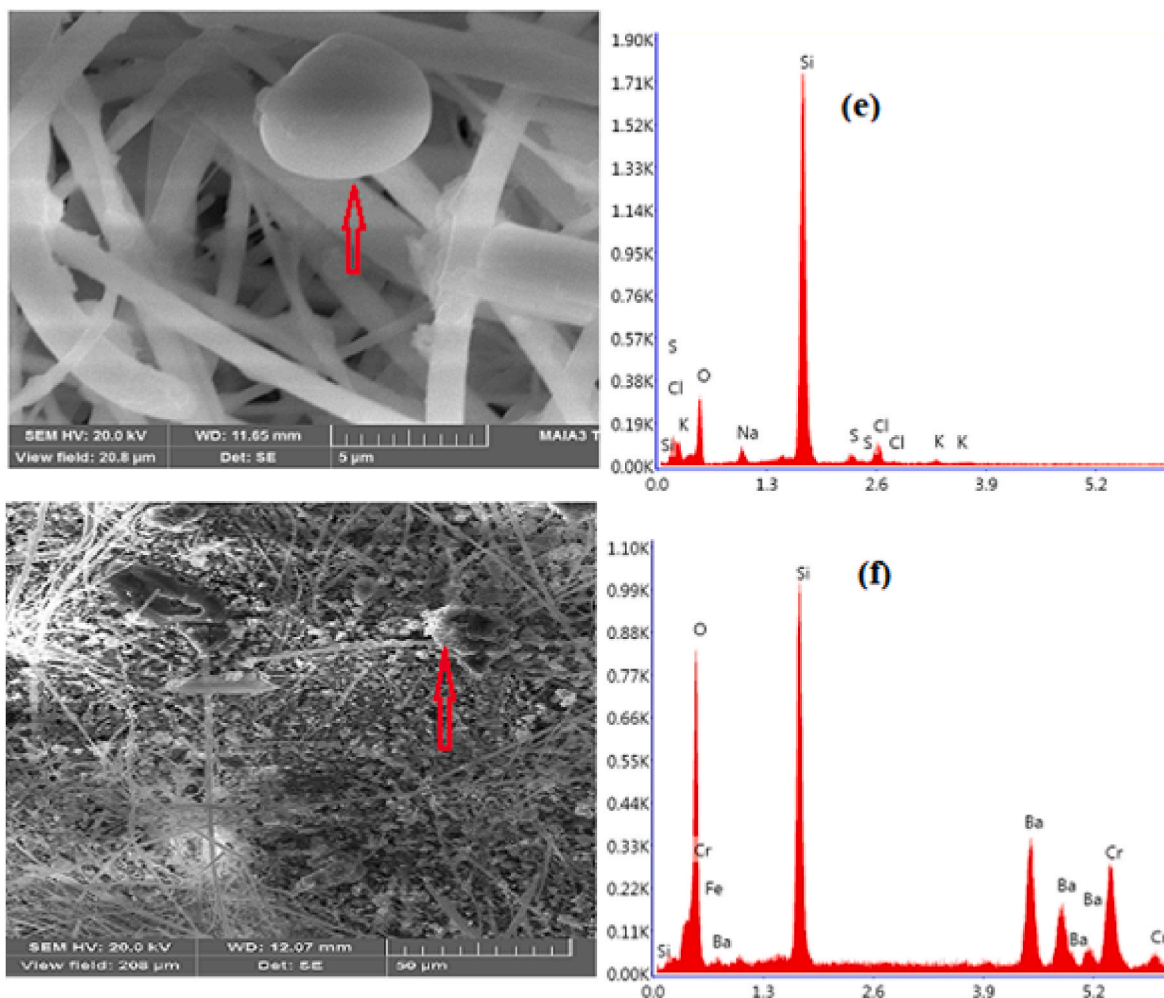
Fig. 8. (*continued*).

quality. Multiple emission sources, including vehicular, industrial, and biomass burning activities, have contributed to forming a considerable haze in the region. Previous reports by Alam et al. (2018) documented a similar super haze episode in 2010 over the Himalayan region, which extended across India and Pakistan. During such episodes, biomass burning and urban/industrial aerosols dominated the aerosol composition. Before and after the haze days over Lahore, a mix of aerosols was observed. Additionally, primary emissions from combustion-related sources, agricultural activities, and biomass burning substantially contribute to the winter increase in PM2.5 concentrations (Li et al., 2021). Urbanization, industrialization, and vehicular emissions have escalated PM2.5 mass concentrations, exacerbating air quality issues in Lahore (Shi et al., 2020). Thermal inversion layers, prevalent during winter, significantly elevate PM2.5 levels (Rasheed et al., 2015). The influence of such atmospheric conditions, compounded by primary emissions from combustion-related activities and biomass burning, exacerbates air pollution, especially during dense fog episodes in Lahore (Zeb et al., 2018; Nagar et al., 2017).

Fig. 4 illustrates the direct correlation between PM2.5 mass concentration and Relative Humidity (RH), while an inverse relationship is observed with temperature and wind speed. RH showed a direct association with PM2.5 concentrations, indicating unfavorable conditions for pollutant dispersion, resulting in heightened pollution levels during winter (Wang et al., 2013). Notably, December recorded a maximum PM2.5 concentration of 301 μgm^{-3} at a lower temperature of 19.1 °C, while October reported a minimum concentration of 30.9 μgm^{-3} at a higher temperature of 26.1 °C. The association between temperature and PM2.5 concentrations aligns with prior research, highlighting a negative correlation between temperature and PM2.5 concentrations during winter (Ye et al., 2003; Raja et al., 2010; Barmpadimos et al., 2012; Zheng et al., 2015). Furthermore, increased wind speed corresponded to decreased PM2.5 concentrations, signifying its role in pollutant dispersion. Higher wind speeds facilitate better pollutant diffusion, while lower speeds result in PM2.5 accumulations near the surface (Zhao et al., 2015; Jiang et al., 2021). These variations in meteorological parameters align with findings reported by Rasheed et al. (2015).

This analysis underscores the intricate relationship between meteorological conditions and PM2.5 concentrations, emphasizing the multifaceted factors contributing to air quality deterioration in Lahore. The present study investigated high level of PM2.5 concentration in the in second largest city of Pakistan i.e. Lahore. The results of the current study will enhance the understanding of the trends of PM2.5 mass concentrations, in the city. Our study underscores the complex interplay of various factors contributing to air quality deterioration in Lahore, including seasonal variations, emission sources, and meteorological influences. These insights hold significant implications for policymakers and urban planners, providing valuable guidance for implementing targeted measures aimed at reducing pollution levels and safeguarding public health.

3.2. Raman analysis

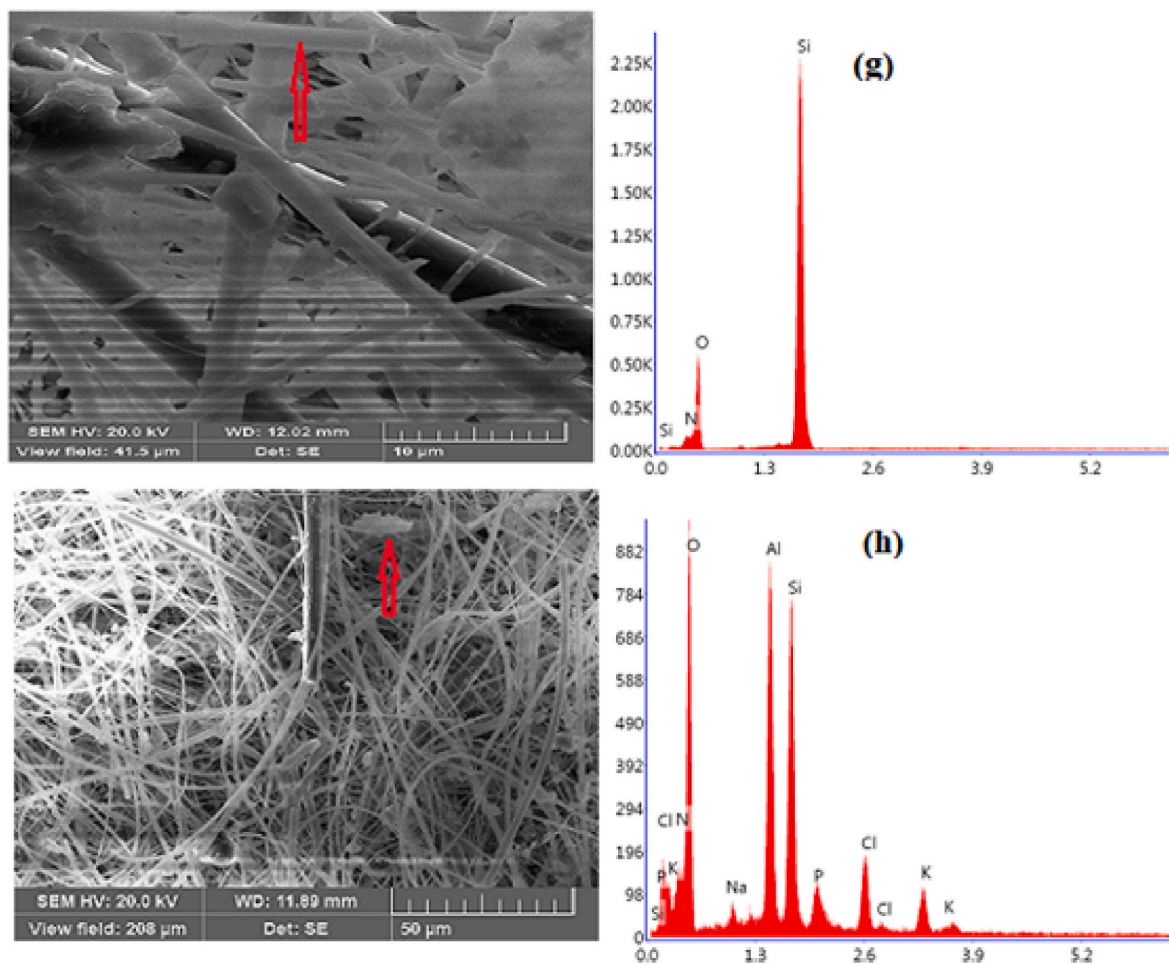In the current study we have exploited Ramman spectroscopy for the

Fig. 8. (*continued*).

determination of minerals and chemical compounds collected aerosols samples during haze event. It provides a fingerprint spectra of each molecular species in organic and inorganic materials. Fig. 5 (a) and 5 (b) present the average Raman intensity plotted against the Raman shift for samples S1 to S10 during the study period. These plots revealed distinct peaks labeled from 1 to 11, each corresponding to specific wavelengths: (1) 461 cm^{-1}, (2) 480 cm^{-1}, (3) 632 cm^{-1}, (4) 720 cm^{-1}, (5) 890 cm^{-1}, (6) 961 cm^{-1}, (7) 990 cm^{-1}, (8) 1053 cm^{-1}, (9) 1090 cm^{-1}, (10) 1388 cm^{-1}, and (11) 1400–1580 cm^{-1}. The Raman analyses conducted on PM2.5 unveiled the presence of several minerals and ions, including calcite, silicate, quartz, phosphate, barite, nitrate, and sulfate ions. The specific peaks at distinct wavelengths indicated the existence of various chemical compounds and minerals. The 461 cm^{-1} peak signifies the presence of quartz minerals (Bower et al., 2016; Yu et al., 2021), while the 480 cm^{-1} peak indicates amorphous silica (Wu et al., 1996). Thenardite salt (Na_2SO_4) was inferred from the characteristic peak at 632 cm^{-1} (Taboada et al., 2019). Additionally, the 890 cm^{-1} peak suggests the occurrence of methane (Li and Renneckar, 2011), and the 990 cm^{-1} peak indicates the presence of barite salt ($BaSO_4$) (Marszałek, 2016).

Phosphate minerals were identified through the peak at 961 cm^{-1} (Desoutter et al., 2014), while the strong peak at 1053 cm^{-1} corresponds to secondary inorganic compounds like $Ca(NO_3)_2.4H_2O$ or $NaNO_3$ (Kloprogge et al., 2002; Ji et al., 2015). The presence of calcite ($CaCO_3$) was detected at 720 cm^{-1} (DeCarlo, 2018) and 1085 cm^{-1} (Raz et al., 2003). The Raman peaks at 1388 cm^{-1} and the range of 1400 cm^{-1}–1580 cm^{-1} indicated the presence of CO_2 and a standard graphitic band, respectively (Angel et al., 2012; Soewono and Rogak, 2011). Furthermore, some samples exhibited minor insignificant peaks. The quartz

minerals, sulfate ions $(SO_4)^{2-}$, and nitrate ions $(NO_3)^-$ originate from various sources such as soil, glass, ceramics, and sedimentary rocks. Sulfate ions predominantly stem from coal, fossil fuels, biomass burning, and agricultural activities (Zeb et al., 2018; Ji et al., 2015). One of the dominant sources for sulfate ions is the fly ash that arrised due to burning of agricultural waste in the vicinity of study area which is the common activity during the study period (Ji et al., 2015). The agricultural burning along with photochemical reaction are the dominant sources of haze formation (Sun et al., 2014). Nitrate ions arise from automobile exhaust, industrial emissions, and fossil fuel combustion, contributing to nitric acid formation, i.e., acid rain (Song et al., 2021). The rapid increase in number of vehicles (>4.2 million) with low quality fuel along with emissions from various industries (about 2700 registered), brick kiln, tailpipes etc., in Lahore are the major sources for accumulation of nitrate ions (Butt et al., 2018; Haider et al., 2018; Asghar, M. Z. 2018).

The presence of $CaCO_3$, a crucial mineral in stone, arises from soil dust, crustal materials, construction, vehicular emissions, and wind-blown dust (Marszałek, 2016; Pachauri et al., 2013). Natural iron-oxide (Fe_2O_3) content in the atmosphere originates from iron-containing mineral dust and anthropogenic activities like fossil fuel burning and combustion (Čabanová et al., 2019; Ji et al., 2015). Additionally, emissions from aluminum production processes, mining, coal combustion, and motor vehicle exhaust contribute to atmospheric aluminum concentration (Rebollo-Plata et al., 2014; Xie et al., 2005). The vehicular emissions, and coal combustions are the major contributor to haze particle during colder days (Sun et al., 2014). The above findings suggest that, the stagnant meteorological condition (section 2.4) such as low

wind speed, lower temperature and deepened boundary layer height during the study period favour the accumulation of the haze pollutant originating from various sources in to the local atmosphere.

3.3. X-ray diffraction measurement and analysis

XRD analysis offers potential for an enhanced investigation into the mineralogical composition of PM2.5 samples, facilitating a better understanding of their sources, atmospheric reactions, and potential health implications. The XRD pattern of PM2.5 samples throughout the study period is illustrated in Fig. 6. The data was plotted based on the Cu Kα line with a wavelength of 1.540 A° (30 kV, 40 mA), spanning an angle 2θ range between 10 and 120°. Notably, the XRD results showcased consistent peaks across all samples. Distinct peaks were observed at specific angles: 12.5°, 21.5°, 37°, 44.4°, 64°, 78°, and 116°, denoted as points 1, 2, 3, 5, 6, and 7, respectively, in the XRD pattern. These peaks corresponded to particular minerals and compounds found in the PM2.5 samples. At 12.5°, a prominent peak indicative of calcium silicate ($CaSiO_3$) was observed, a finding consistent with Wu et al. (2007). Similarly, the presence of minerals such as ammonium sulfate ((NH_4)$_2SO_4$) at 21.5° and hematite (Fe_2O_3) at 37° aligns with previous research by Usman et al. (2022). The identification of gypsum ($CaSO_4.2H_2O$) at 44.4° in the XRD data is in agreement with the observations reported by Tiwari et al. (2016) and Hamdan et al. (2016), respectively. Furthermore, the characteristic peaks of calcite ($CaCO_3$) at 64° correspond to findings documented by Melki et al. (2017). Additionally, the presence of quartz mineral was confirmed by a peak at 78°, along with a smaller peak at 116°, consistent with previous identifications reported by Neupane et al. (2020). These consistent XRD peaks denote the presence of specific minerals and compounds within the PM2.5 samples collected during the study period which supports the finding in section 3.2.

3.4. SEM-EDX results and analysis

The constituent elements present in the PM2.5 filter samples are depicted in Fig. 7, as revealed by EDX spectroscopy. Nineteen elements were identified: C, N, O, Na, Mg, Al, Si, S, Cl, K, Ca, Fe, Zn, Ba, Ni, As, P, Cr, and Pb. Of these elements, the weight percentages of carbon (C), nitrogen (N), and oxygen (O) were notably higher compared to the others. The presence of carbon, sulfur, nitrogen, potassium, and zinc in the samples can be attributed to various sources, including fossil fuel combustion, biomass burning, vehicular emissions, and agricultural activities in the study area (Demirbas, 2005). Additionally, oxygen, sodium, magnesium, silicon, calcium, and iron were detected, likely originating from traffic emissions, construction activities, and clay minerals prevalent in the area (Zeb et al., 2022). Industrial pollutants such as chromium, nickel, phosphorus, and arsenic were also found as trace elements in the samples, suggesting diverse sources contributing to crustal and trace metals in the region.

Moreover, our study identified trace amounts of contaminated heavy metals, specifically barium and lead. The presence of lead, associated with the metal industry, waste incinerators, battery manufacturing (Borah et al., 2020), and road traffic emissions (Radulescu et al., 2017), was recorded. Barium, attributable to industrial activities involving cutting, mining, refining of barium-based chemicals, fossil fuel combustion, and natural sources like soil and rock dust, was also detected in the environment (Koukoulakis et al., 2019; Ryder et al., 2020). These findings suggest a multitude of sources contributing to the presence of various elements and heavy metals in the PM2.5 samples collected, underscoring the complexity and diverse origins of air pollutants in the studied. The exposure to such type of haze chemistry may leads to vulnerabe health symptoms such as breathing difficulty, eye and throat discomfort, respiratory morbidity, and even cardiovascular mortality (Ramakreshnan et al., 2018).

The SEM micrographs and selected regions' EDX spectra of PM2.5 particles are presented in Fig. 8(a–h). The images illustrate the composition and morphology of the particles observed during this study. The majority of particles appear to be aggregates of smaller particles without defined morphology, indicating complex structures. Fig. 8(a) depicts micrographs of a blank quartz fiber filter paper. These filters, primarily composed of silicon and oxygen, serve as effective substrates for collecting particulate matter (Casuccio et al., 2004). Within the particle group, Fig. 8(b) displays irregularly shaped almandine ($Fe_3Al_2(SiO_4)_3$). Almandine, a type of aluminosilicate, is commonly derived from soil and exhibits compositions of silicon and aluminum oxides along with various elements like Na, K, Mg, Ca, and Fe. These aluminosilicates constitute a significant portion of chemical compounds found in the Earth's crust, often originating from sources such as agriculture activities, resuspended dust, rocks, and construction activities (Pachauri et al., 2013; Zeb et al., 2018). Different variations of aluminosilicate particles, including irregularly shaped Ca–Mg aluminosilicate particles (Fig. 8(c)) and Aluminosilicate particles (Fig. 8(h)), were identified in this study. Kim et al. (2018) also reported similar sources for aluminosilicates, linking them to soil deposits, dust, biomass burning, fossil fuel combustion, and other combustion activities (Roberts et al., 2019). Carbonaceous particles, originating from fossil fuel combustion, biomass burning, coal, and vehicular emissions (Stone et al., 2010), exhibited diverse morphologies ranging from soot to more complex structures. In our observations, these particles appeared as aggregated chains (Fig. 8 (d)).

Fig. 8(e) showcases sulfate particles exhibiting capsule-like symmetry. These sulfur-related particles are primarily generated from sulfur dioxide emissions during heavy-duty vehicle fuel combustion (Lu et al., 2011). They can also stem from soil dust, crustal resuspension, and various anthropogenic sources like construction, vehicular emissions, combustion, and agricultural activities (Bisht et al., 2022). Barium particles with octahedral morphology are illustrated in Fig. 8(f). These particles, are predominantly emitted from coal, sandstone, igneous rocks (Niu et al., 2018), and industrial processes involved in refining and mining of barium-based chemicals (Koukoulakis et al., 2019). Lastly, Fig. 8(g) shows columnar-shaped nitrogenous particles. The primary sources of nitrogen emissions in the study site were found to be agricultural activities and the decomposition of organic matter from plants and animals (Carpenter et al., 1998).

4. Conclusion

The analysis of PM2.5 samples has revealed a diverse array of minerals and ions, indicative of the myriad emission sources contributing to air pollution in Lahore. Notably, biomass burning, industrial emissions, vehicular exhaust, and natural sources such as soil dust collectively contribute to the complex chemical composition of PM2.5. These findings underscore the imperative for targeted interventions aimed at mitigating pollution sources and ameliorating air quality in the region.

The findings highlight alarming levels of PM2.5 concentrations, surpassing WHO standards, indicating severe air quality deterioration in the region. The primary sources contributing to elevated PM2.5 concentrations include biomass burning, agricultural residue incineration, vehicular emissions, and industrial activities. Raman spectroscopy and X-ray diffraction techniques were instrumental in identifying the diverse composition of PM2.5, revealing the presence of quartz minerals, sulfate, nitrate, aluminosilicates, and various heavy metals like lead, barium, chromium, and nickel. The Ramman spectroscopy is scarsly used in the charactarization of particulate matter and this techniques may be ascribed to the possibility of a massive enrichment in the intensity of Raman signals, commanding better characterization. It presents an opportunity for deeper exploration into the chemical composition and molecular structure of PM2.5 constituents, offering valuable information on their origin and transformation processes. However, greater sophistication in the instrumentation and more advanced technology will surely pave the way toward a better intellect

of the complexity of aerosol measurements.

SEM-EDX analysis further elucidated the complex morphology and diverse elemental composition of the collected PM2.5 particles, showcasing aggregates with no defined morphology, aluminosilicates derived from soil, carbonaceous particles from combustion sources, sulfate particles from vehicular emissions, industrial pollutants like barium, and nitrogenous particles from organic matter decomposition. These respirable particles (PM2.5) may penetrate the respiratory system and cause asthma, cardiovascular or lung disease. Our study does not explore certain aspects such as visibility, health, and environmental or socio-economic impacts of air pollution, which could be avenues for future research. The meteorological conditions, especially humidity and wind speed, displayed a direct and inverse relationship, respectively, with PM2.5 concentrations. Temperature inversely correlated with PM2.5 levels, indicating the trapping of particles due to minimal temperature inversion during winter.

While our findings align with prior research on PM2.5 composition and sources in urban environments, we acknowledge the necessity for further in-depth analysis to uncover unique insights specific to Lahore's air pollution context. Although similar trends in PM2.5 concentrations and meteorological influences have been documented in other regions, the distinct characteristics of Lahore's air pollution necessitate advanced examination to devise tailored solutions for effective pollution control and management. It is important to note the limitations of our study. Our analysis provides a snapshot of air pollution conditions during the study period and may not capture long-term trends or specific localized variations. Additionally, this study does not explore certain aspects such as pollutant transport mechanisms or the socio-economic impacts of air pollution, which could be avenues for future research. Long-term monitoring studies, along with source apportionment analyses, can provide deeper insights into the dynamics of air pollution and aid in the formulation of targeted interventions for sustainable air quality improvement in the region. Additionally, studies exploring the health impacts of these diverse PM2.5 compositions on the local population would further enhance our understanding of the health risks associated with air pollution in Lahore. Policymakers can use such types of inviatigation in developing effective air pollution management plans, establishing efficient compliance monitoring, performing epidemiological health research, and putting in place a health warning system in Lahore.

Ethical approval

The manuscript is not submitted to other journal for simultaneous consideration.

Availability of data and materials

The data will be available on request from the corresponding author.

Funding

No funding was received for conducting this study.

CRediT authorship contribution statement

Saima Mohyuddin: Writing – original draft, Conceptualization. **Khan Alam:** Writing – review & editing, Conceptualization. **Bahadar Zeb:** Methodology. **Muhammad Fahim Khokhar:** Formal analysis. **Kaleem Anwar Mir:** Writing – review & editing. **Anthony S. Wexler:** Writing – review & editing. **Ehtiram ul Haq:** Methodology. **Muhammad Ikram:** Supervision. **Imran Shahid:** Validation, Supervision.

Declaration of competing interest

The authors declare that they have no known competing financial interests or personal relationships that could have appeared to influence the work reported in this paper.

Data availability

No data was used for the research described in the article.

References

Ahmad, M., Yu, Q., Chen, J., Cheng, S., Qin, W., Zhang, Y., 2021. Chemical characteristics, oxidative potential, and sources of PM2. 5 in wintertime in Lahore and Peshawar, Pakistan. J. Environ. Sci. 102, 148–158.

Alam, K., Khan, R., Sorooshian, A., Blaschke, T., Bibi, S., Bibi, H., 2018. Analysis of aerosol optical properties due to a haze episode in the Himalayan foothills: implications for climate forcing. Aerosol Air Qual. Res. 18 (5), 1331–1350.

Alam, K., Mukhtar, A., Shahid, I., Blaschke, T., Majid, H., Rahman, S., et al., 2014. Source apportionment and characterization of particulate matter (PM10) in urban environment of Lahore. Aerosol Air Qual. Res. 14 (7), 1851–1861.

Angel, S.M., Gomer, N.R., Sharma, S.K., McKay, C., 2012. Remote Raman spectroscopy for planetary exploration: a review. Appl. Spectrosc. 66 (2), 137–150.

Asghar, M.Z., 2018. Comparative assessment of physico-chemical parameters of waste water effluents from different industries in Lahore, Pakistan. Proc. Int. Aca. Ecol. Environ. Sci. 8 (2), 99.

Bari, M.A., Kindzierski, W.B., 2016. Fine particulate matter (PM2. 5) in Edmonton, Canada: source apportionment and potential risk for human health. Environ. Pollut. 218, 219–229.

Barmpadimos, I., Keller, J., Oderbolz, D., Hueglin, C., Prévôt, A.S.H., 2012. One decade of parallel fine (PM 2.5) and coarse (PM 10–PM 2.5) particulate matter measurements in Europe: trends and variability. Atmos. Chem. Phys. 12 (7), 3189–3203.

Bisht, L., Gupta, V., Singh, A., Gautam, A.S., Gautam, S., 2022. Heavy metal concentration and its distribution analysis in urban road dust: a case study from most populated city of Indian state of Uttarakhand. Spatial Spatio-temporal Epidemiol. 40, 100470.

Borah, P., Kumar, M., Devi, P., 2020. Types of Inorganic Pollutants: Metals/metalloids, Acids, and Organic Forms. Elsevier, pp. 17–31.

Bower, D.M., Steele, A., Fries, M.D., Green, O.R., Lindsay, J.F., 2016. Raman imaging spectroscopy of a putative microfossil from the~ 3.46 Ga Apex chert: insights from quartz grain orientation. Astrobiology 16 (2), 169–180.

Butt, M.T., Abbas, N.A.E.E.M., Deeba, F.A.R.A.H., Iqbal, J.A.V.E.D., Hussain, N.A.Q.I., Khan, R.A., 2018. Study of exhaust emissions from different fuels based vehicles in Lahore City of Pakistan. Asian J. Chem. 30 (11), 2481–2485.

Čabanová, K., Hrabovská, K., Matějková, P., Dědková, K., Tomášek, V., Dvořáčková, J., Kukutschová, J., 2019. Settled iron-based road dust and its characteristics and possible association with detection in human tissues. Environ. Sci. Pollut. Control Ser. 26 (3), 2950–2959.

Cardell, C., Guerra, I., 2016. An overview of emerging hyphenated SEM-EDX and Raman spectroscopy systems: applications in life, environmental and materials sciences. TrAC, Trends Anal. Chem. 77, 156–166.

Carpenter, S.R., Caraco, N.F., Correll, D.L., Howarth, R.W., Sharpley, A.N., Smith, V.H., 1998. Nonpoint pollution of surface waters with phosphorus and nitrogen. Ecol. Appl. 8 (3), 559–568.

Carrero, J.A., Arana, G., Madariaga, J.M., 2014. Use of Raman spectroscopy and scanning electron microscopy for the detection and analysis of road transport pollution. Spectrosc. Prop. Inorg. Organomet. C 45, 178–210.

Casuccio, G.S., Schlaegle, S.F., Lersch, T.L., Huffman, G.P., Chen, Y., Shah, N., 2004. Measurement of fine particulate matter using electron microscopy techniques. Fuel Process. Technol. 85 (6–7), 763–779.

Che, W., Zhang, Y., Lin, C., Fung, Y.H., Fung, J.C., Lau, A.K., 2023. Impacts of pollution heterogeneity on population exposure in dense urban areas using ultra-fine resolution air quality data. Environ. Sci. J. Integr. Environ. Res. 125, 513–523.

DeCarlo, T.M., 2018. Characterizing coral skeleton mineralogy with Raman spectroscopy. Nat. Commun. 9 (1), 5325.

Demirbas, A., 2005. Potential applications of renewable energy sources, biomass combustion problems in boiler power systems, and combustion-related environmental issues. Prog. Energy Combust. Sci. 31 (2), 171–192.

Desoutter, A., Salehi, H., Slimani, A., Marquet, P., Jacquot, B., Tassery, H., Cuisinier, F.J. G., 2014. Structure and chemical composition of the dentin-enamel junction analyzed by confocal Raman microscopy. SPIE 8929, 49–56.

Dominici, F., Peng, R.D., Bell, M.L., Pham, L., McDermott, A., Zeger, S.L., Samet, J.M., 2006. Fine particulate air pollution and hospital admission for cardiovascular and respiratory diseases. J. Am. Med. Assoc. 295 (10), 1127–1134.

Hamdan, N.M., Alawadhi, H., Jisrawi, N., 2016. Particulate matter pollution in the United Arab Emirates: elemental analysis and phase identification of fine particulate pollutants. Budapest 18–19.

Haider, R., Yasar, A., Tabinda, A.B., 2018. Impact of transport sustainability on air quality in Lahore, Pakistan. Curr. Sci. 2380–2386. https://www.airscan.org/en/news/who2021.

Inerb, M., Phairuang, W., Paluang, P., Hata, M., Furuuchi, M., Wangpakapattanawong, P., 2022. Carbon and trace element compositions of total suspended particles (TSP) and nanoparticles (PM0.1) in ambient air of southern Thailand and characterization of their sources. Atmosphere 13. https://doi.org/10.3390/atmos13040626.6392.

Ji, Z., Dai, R., Zhang, Z., 2015. Characterization of fine particulate matter in ambient air by combining TEM and multiple spectroscopic techniques–NMR, FTIR, and Raman spectroscopy. Environ. Sci. J. Integr. Environ. Res. 17 (3), 552–560.

Jiang, Z., Cheng, H., Zhang, P., Kang, T., 2021. Influence of urban morphological parameters on the distribution and diffusion of air pollutants: a case study in China. J. Environ. Sci. 105, 163–172.

Jin, M., Shepherd, J.M., King, M.D., 2005. Urban aerosols and their variations with clouds and rainfall: a case study for New York and Houston. J. Geophys. Res. Atmos. 110.

Kim, W., Shin, J.Y., Hyeong, K., Lee, T., Kim, T.H., 2018. Particulate pollution by biomass burning using environmental magnetic assessment of grain-size fractioned wet-deposits in Korea. American Geophysical Union 43C-0794.

Kloprogge, J.T., Wharton, D., Hickey, L., Frost, R.L., 2002. Infrared and Raman study of interlayer anions (CO32-)-1, (NO3)-1, (SO4)-2, and (ClO4)-1 in Mg/Al-hydrotalcite. Am. Mineral. 87 (5–6), 623–629.

Kobza, J., Geremek, M., Dul, L., 2018. Characteristics of air quality and sources affecting high levels of PM10 and PM2. 5 in Poland, Upper Silesia urban area. Environ. Monit. Assess. 190 (9), 1–13.

Koukoulakis, K.G., Chrysohou, E., Kanellopoulos, P.G., Karavoltsos, S., Katsouras, G., Dassenakis, M., et al., 2019. Trace elements bound to airborne PM10 in a heavily industrialized site nearby Athens: seasonal patterns, emission sources, health implications. Atmos. Pollut. Res. 10 (4), 1347–1356.

Kumar, S., Prasad, S., Yadav, K.K., 2019. Utilization of air pollutants by plants. Agricul. Food Chem. 67 (10), 2741–2742.

Lee, M., 2017. X-Ray Diffraction for Materials Research, vol. 13. Apple Academic Press.

Li, F., Gu, J., Xin, J., Schnelle-Kreis, J., Wang, Y., Liu, Z., et al., 2021. Characteristics of the chemical profile, sources, and PAH toxicity of PM2. 5 in Beijing in autumn-winter transition season about domestic heating, pollution control measures, and meteorology. Chemosphere 276, 130143.

Li, Q., Renneckar, S., 2011. Supramolecular structure characterization of molecularly thin cellulose I nanoparticles. Biomacromolecules 12 (3), 650–659.

Lu, Z., Zhang, Q., Streets, D.G., 2011. Sulfur dioxide and primary carbonaceous aerosol emissions in China and India, 1996–2010. Atmos. Chem. Phys. 11 (18), 9839–9864.

Marszałek, M., 2016. Identification of secondary salts and their sources in deteriorated stone monuments using micro-Raman spectroscopy, SEM-EDX, and XRD. J. Raman Spectrosc. 47 (12), 1473–1485.

Melki, P.N., Ledoux, F., Aouad, S., Billet, S., El Khoury, B., Landkocz, Y., et al., 2017. Physicochemical characteristics, mutagenicity, and genotoxicity of airborne particles under industrial and rural influences in Northern Lebanon. Environ. Sci. Pollut. Control Ser. 24 (23), 18782–18797.

Mir, K.A., Purohit, P., Cail, S., Kim, S., 2022. Co-benefits of air pollution control and climate change mitigation strategies in Pakistan. Environ. Sci. Pol. 133, 31–43.

Mir, K.A., Purohit, P., Ijaz, M., Babar, Z.B., Mehmood, S., 2023. Black carbon emissions inventory and scenario analysis for Pakistan. Environ. Pollut. 340, 122745.

Nagar, P.K., Singh, D., Shasxrma, M., Kumar, A., Aneja, V.P., George, M.P., et al., 2017. Characterization of PM2. 5 in Delhi: role and impact of secondary aerosol, burning of biomass, and municipal solid waste and crustal matter. Environ. Sci. Pollut. Control Ser. 24 (32), 25179–25189.

Neupane, B.B., Sharma, A., Giri, B., Joshi, M.K., 2020. Characterization of airborne dust samples collected from core areas of Kathmandu Valley. Heliyon 6 (4), e03791.

Nihalani, S.A., Khambete, A.K., Jariwala, N.D., 2020. Review of Source Apportionment of Particulate Matter for Indian Scenario, vol. 61. Springer, pp. 209–218.

Niu, X., Wendt, A., Li, Z., Agarwal, A., Xue, L., Gonzales, M., Brantley, S.L., 2018. Detecting the effects of coal mining, acid rain, and natural gas extraction in Appalachian basin streams in Pennsylvania (USA) through analysis of barium and sulfate concentrations. Environ. Geochem. Health 40 (2), 865–885.

Olawoyin, R., Schweitzer, L., Zhang, K., Okareh, O., Slates, K., 2018. Index analysis and human health risk model application for evaluating ambient air-heavy metal contamination in Chemical Valley Sarnia. Ecotoxicol. Environ. Saf. 148, 72–81.

Pachauri, T., Singla, V., Satsangi, A., Lakhani, A., Kumari, K.M., 2013. SEM-EDX characterization of individual coarse particles in Agra, India. Aerosol Air Qual. Res. 13 (2), 523–536.

Park, S.S., Kim, Y.J., 2005. Source contributions to fine particulate matter in an urban atmosphere. Chemosphere 59 (2), 217–226.

Pun, V.C., Kazemiparkouhi, F., Manjourides, J., Suh, H.H., 2017. Long-term PM2. 5 exposure and respiratory, cancer, and cardiovascular mortality in older US adults. Am. J. Epidemiol. 186 (8), 961–969.

Radulescu, C., Stihi, C., Iordache, S., Dunea, D., Dulama, I.D., 2017. Characterization of urban atmospheric PM2. 5 by ATR-FTIR, ICP-MS and SEM-EDS techniques. Rev. Chem. 68 (4), 805–810.

Raja, S., Biswas, K.F., Husain, L., Hopke, P.K., 2010. Source apportionment of the atmospheric aerosol in Lahore, Pakistan. Water Air Soil Pollut. 208, 43–57.

Ramakreshnan, L., Aghamohammadi, N., Fong, C.S., Bulgiba, A., Zaki, R.A., Wong, L.P., Sulaiman, N.M., 2018. Haze and health impacts in ASEAN countries: a systematic review. Environ. Sci. Pollut. Control Ser. 25, 2096–2111.

Ramanathan, V., Chung, C., Kim, D., Bettge, T., Buja, L., Kiehl, J.T., et al., 2005. Atmospheric brown clouds: impacts on South Asian climate and hydrological cycle. Proc. Natl. Acad. Sci. USA 102 (15), 5326–5333.

Rani, B., Singh, U., Chuhan, A.K., Sharma, D., Maheshwari, R., 2011. Photochemical smog pollution and its mitigation measures. J. Adv. Sci. Res. 2 (4), 28–33.

Rasheed, A., Aneja, V.P., Aiyyer, A., Rafique, U., 2015. Measurement and analysis of fine particulate matter (PM2. 5) in urban areas of Pakistan. Aerosol Air Qual. Res. 15 (2), 426–439.

Raz, S., Hamilton, P.C., Wilt, F.H., Weiner, S., Addadi, L., 2003. The transient phase of amorphous calcium carbonate in sea urchin larval spicules: the involvement of proteins and magnesium ions in its formation and stabilization. Adv. Funct. Mater. 13 (6), 480–486.

Rebollo-Plata, B., Sampedro, M.P., Gallardo-Gómez, G., Ortega-Miranda, N., Bravo-Barrera, C.F., Daniel-Pérez, G., et al., 2014. Growth of metal micro and/or nanoparticles utilizing arc-discharge immersed in liquid. Rev. Mexic. Fisica 60 (3), 227–232.

Ristovski, Z.D., Miljevic, B., Surawski, N.C., Morawska, L., Fong, K.M., Goh, F., Yang, I. A., 2012. Respiratory health effects of diesel particulate matter. Respirology 17 (2), 201–212.

Roberts, L.J., Mason, P.E., Jones, J.M., Gale, W.F., Williams, A., Ashman, J., 2019. The impact of aluminosilicate-based additives upon the sintering and melting behavior of biomass ash. Biomass Bioenergy 127, 105284.

Rodríguez, S., Querol, X., Alastuey, A., Plana, F., 2002. Sources and processes affecting levels and composition of atmospheric aerosol in the western Mediterranean. J. Geophys. Res. Atmos. 107, 12.

Ryder, O.S., DeWinter, J.L., Brown, S.G., Hoffman, K., Frey, B., Mirzakhalili, A., 2020. Assessment of particulate toxic metals at an Environmental Justice community. Atmos. Environ. 6, 100070.

Samae, H., Tekasakul, S., Tekasakul, P., Furuuchi, M., 2021. Emission factors of ultrafine particulate matter (PM<0.1 mum) and particle-bound polycyclic aromatic hydrocarbons from biomass combustion for source apportionment. Chemosphere 262, 641127846. https://doi.org/10.1016/j.chemosphere.2020.127846.642.

Shi, Y., Bilal, M., Ho, H.C., Omar, A., 2020. Urbanization and regional air pollution across South Asian developing countries–A nationwide land use regression for ambient PM2.5 assessments in Pakistan. Environ. Pollut. 266, 115145.

Singh, R.P., Kaskaoutis, D.G., 2014. Crop residue burning: a threat to South Asian air quality. Eos, Transactions American Geophysical Union 95 (37), 333–334.

Soewono, A., Rogak, S., 2011. Morphology and Raman spectra of engine-emitted particulates. Aerosol. Sci. Technol. 45 (10), 1206–1216.

Song, W., Liu, X.Y., Hu, C.C., Chen, G.Y., Liu, X.J., Walters, W.W., et al., 2021. Important contributions of non-fossil fuel nitrogen oxides emissions. Nat. Commun. 12 (1), 243.

Stone, E., Schauer, J., Quraishi, T.A., Mahmood, A., 2010. Chemical characterization and source apportionment of fine and coarse particulate matter in Lahore, Pakistan. Atmos. Environ. 44 (8), 1062–1070.

Sun, Y., Jiang, Q., Wang, Z., Fu, P., Li, J., Yang, T., Yin, Y., 2014. Investigation of the sources and evolution processes of severe haze pollution in Beijing in January 2013. J. Geophys. Res. Atmos. 119 (7), 4380–4398.

Taboada, N.P., Vallejuelo, S.F.O., Veneranda, M., Lama, E., Castro, K., Arana, G., et al., 2019. The Raman spectra of the Na2SO4-K2SO4 system: applicability to soluble salts studies in built heritage. J. Raman Spectrosc. 50 (2), 175–183.

Tiwari, G., Brahme, N., Sharma, R., Bisen, D.P., Sao, S.K., Tigga, S., 2016. Luminescence properties of dysprosium doped di-calcium di-aluminum silicate phosphors. Opt. Mater. 58, 234–242.

Usman, F., Zeb, B., Alam, K., Huang, Z., Shah, A., Ahmad, I., Ullah, S., 2022. In-depth analysis of physicochemical properties of particulate matter (PM10, PM2. 5 and PM1) and its characterization through FTIR, XRD, and SEM–EDX techniques in the foothills of the hindu kush region of northern Pakistan. Atmosphere 13 (1), 124.

Vernon-Parry, K.D., 2000. Scanning electron microscopy: an introduction. III-Vs Rev. 13 (4), 40–44.

Wang, J., Wang, Y., Liu, H., Yang, Y., Zhang, X., Li, Y., et al., 2013. Diagnostic identification of the impact of meteorological conditions on PM2. 5 concentrations in Beijing. Atmos. Environ. 81, 158–165.

Wang, Z., Zhong, S., Peng, Z.R., Cai, M., 2018. Fine-scale variations in PM2. 5 and black carbon concentrations and corresponding influential factors at an urban road intersection. Build. Environ. 141, 215–225.

Wu, C., Ramaswamy, Y., Kwik, D., Zreiqat, H., 2007. The effect of strontium incorporation into CaSiO3 ceramics on their physical and biological properties. Biomaterials 28 (21), 3171–3181.

Wu, X.L., Siu, G.G., Tong, S., Liu, X.N., Yan, F., Jiang, S.S., et al., 1996. Raman scattering of alternating nanocrystalline silicon/amorphous silicon multilayers. Appl. Phys. Lett. 69 (4), 523–525.

Xie, R.K., Seip, H.M., Leinum, J.R., Winje, T., Xiao, J.S., 2005. Chemical characterization of individual particles (PM10) from ambient air in Guiyang City, China. Sci. Total Environ. 343 (1–3), 261–272.

Ye, B., Ji, X., Yang, H., Yao, X., Chan, C.K., Cadle, S.H., et al., 2003. Concentration and chemical composition n of PM2. 5 in Shanghai for a 1-year period. Atmos. Environ. 37 (4), 499–510.

Yu, J., Zhang, C., Wu, W., Cai, Y., Zhang, Y., 2021. Nodes-connected silicon-carbon nanofibrous hybrids anodes for lithium-ion batteries. Appl. Surf. Sci. 548, 148944.

Zeb, B., Alam, K., Ditta, A., Ullah, S., Ali, H.M., Ibrahim, M., Salem, M.Z., 2022. Variation in coarse particulate matter (PM10) and its characterization at multiple locations in the semiarid region. Front. Environ. Sci. 36.

Zeb, B., Alam, K., Sorooshian, A., Blaschke, T., Ahmad, I., Shahid, I., 2018. On the morphology and composition of particulate matter in an urban environment. Aerosol Air Qual. Res. 18 (6), 1431.

Zhang, R., Wang, G., Guo, S., Zamora, M.L., Ying, Q., Lin, Y., et al., 2015. Formation of urban fine particulate matter. Chem. Rev. 115 (10), 3803–3855.

Zhao, L., Chen, C., Wang, P., Chen, Z., Cao, S., Wang, Q., et al., 2015. Influence of atmospheric fine particulate matter (PM2. 5) pollution on the indoor environment during winter in Beijing. Build. Environ. 87, 283–291.

Zheng, G.J., Duan, F.K., Su, H., Ma, Y.L., Cheng, Y., Zheng, B., et al., 2015. Exploring the severe winter haze in Beijing: the impact of synoptic weather, regional transport, and heterogeneous reactions. Atmos. Chem. Phys. 15 (6), 2969–2983.